Proceedings of 2019 IEEE
International Conference on Mechatronics and Automation
August 4 - 7, Tianjin, China

Evaluation Method of Linear Displacement Precision for a Rope-driven Vascular Intervention Surgery Robot

Wei Zhou [1], Shuxiang Guo[1,2]*, Xianqiang Bao[1], Yangming Guo[1]
1 Key Laboratory of Convergence Biomedical Engineering System and Healthcare Technology, The Ministry of Industry and Information Technology, School of Life Science, Beijing Institute of Technology, No.5, Zhongguancun South Street, Haidian District, Beijing 100081, China
2 Faculty of Engineering, Kagawa University, 2217-20 Hayashi-cho, Takamatsu, Kagawa 760-8521, Japan
E-Mails: {zhouwei & guoshuxiang &baoxianqiang & guoyangming} @bit.edu.cn;
** Corresponding author*

***Abstract* - Vascular Intervention Surgery (VIS) becomes more and more popular to diagnosis and treat the cardio-cerebrovascular diseases. This way has many advantages, such as: shorter operation time, less trauma, shorter recovery time and so on. However, this way also has threatened the doctor by ionizing radiation. Therefore, using a robot to assist doctor to undergo surgery appeals to many scholars. And about the robot, the displacement precision is very important in the surgery. In this paper, in order to improve the linear displacement precision of the slave manipulator, the evaluation method for linear displacement precision are proposed. Firstly, the linear displacement model of rope-driven for VIS is established. Secondly, the performance of this model is evaluated by experiments. Lastly, a compensation model is proposed, and this model can effectively improve the linear displacement precision.**

***Index Terms* - vascular intervention surgery, linear displacement precision, displacement model, compensation model, rope driven**

I. INTRODUCTION

Cardio-cerebrovascular diseases are characterized by high disability rate and high mortality rate, which seriously threaten human health [1], [2]. Some surgical methods have been paid closely attention to treating and diagnosing the diseases. Vascular intervention surgery (VIS) is the most widely applied and highly mature techniques for the treatment of the diseases, which helps more and more patients to continue their lives [3]. In traditional VIS, doctors wear 20kg lead protective clothing and undergo surgery under the visual feedback of DSA angiography. This procedure seriously threatens doctors, such as a large amount of ionizing radiation during the operations and spinal injury caused by wearing a heavy lead suit for a long time [4]. Therefore, many attentions have been paid to the research of related medical devices. And several kinds of assisted surgical robots with master-slave structure has been developed. These devices will not only solve the above problems, but also be safer and more reliable. Nowadays, some companies and university scholars have carried out researches on assisted vascular intervention robot. CorPath 200 and CorPath GRX vascular robotic systems (Corindus Vascular Robotics company) have demonstrated safety and efficacy in vascular and endovascular surgery [5]. Kundong Wang of Shanghai Jiao Tong University developed a master-slave robotic system, and the displacement and moving speed of this system are controlled by PID control method. This system's efficiency was successfully validated by animal experiments. However, the developed master-slave robotic system is lack of force feedback [6]. Yu Song et al also developed a master-slave robotic system with force feedback which is achieved by using magnetorheological fluid (MRF), and propulsion structure of the slave site was used to achieve transmission of the catheter [7]. Hao Shen et al only developed a salve robot, which can achieve the injection of contrast agent and the movement of guide wire/guide catheter. And the verification experiment of pig's femoral artery to its carotid artery has been successfully completed [8]. Xianqiang Bao et al developed a novel slave robot, and the theory and method of cooperative operation of guide wire and catheter are put forward, at the same time, the measurement and compensation method of force during operation are also put forward, which largely improved precision of operation, and the effectiveness of the salve robot is verified by clinical trial [9]-[11]. In our previous researches, the multi-generational robotic systems were developed, including moving theory, operating force detecting, the force feedback using MRF, the VR simulator development, unstructured surgical state perception and navigation and so on [12]-[21]. These devices further improve the operation precision of the remote master-slave robotic system. Mohammad Ali Tavallaei and others also have developed the tele-operated robotic system, which can make full use of the patient's clinical experience and operate the catheter directly [22].

High precision control of the position is a very important issue for tele-operated VIS with master-slave robotic system. In order to improve the linear displacement precision, this paper analyses the kinematics characters of propulsion system of the slave manipulator during the guide wire and catheter operated, and the linear displacement mathematical model is established, and a compensation algorithm is proposed according to the error of the experimental results. The remaining of this paper are organized as follows: In section II, the structure of master-slave robotic system is introduced. In section III, the linear displacement model is established. In section IV, experiments and results, and an improved method is proposed. In section V, conclusions and future works are presented.

II. Master-slave Robotic System

Master-slave robotic system has three parts: master manipulator, slave manipulator and communication. And there are guide wire and catheter propulsion system in the slave manipulator, which will be controlled by master manipulator through the communication network based on the TCP/IP protocol. In this system, doctor will operate the master manipulator in a safe room without ion radiation, and the slave manipulator replicates the master manipulator's movement to operate the guide wire and catheter to diagnose and treat the patient's diseases in operating room. During above operations, force information and visual information are collected by salve side and transmitted to the master side. And the force information and visual information are collected by the force sensor and camera respectively. The doctor can undergo surgery safely and availably when assisted by these two kinds of information. And this system efficiently reduces the ion radiations and the injury to the spine. The overall structure of the master-slave VIS robotic system is shown in Fig.1, which was presented in our lab's published paper [10].

A. Master manipulator

The master manipulator is operated directly by doctor, which is used to emit the introductions to the salve side, including the size and direction of linear displacement and the angle of rotation. So the master manipulator is the initiating side of the whole movement. The master manipulator usually includes two operating platforms (Touch X, Geomagic), as shown in Fig.2, which is used to control guide wire and catheter respectively. This platform includes two degrees of freedom, one is rotatory and the other is stretching. And the rotation for upper arms and lower arms of the platform are used to control the rotatory and stretching movement of the guide wire or catheter respectively. However, limited of the motion range, there is a button on the lower arm, which is used to stop the current motion. When this button is pressed down, it means that a new motion circulation will start. In addition, there is force feedback function in this platform, which is presented by the resistance when the force is transmitted from the slave side. And the resistance signal is stronger, the resistance performance is more obvious.

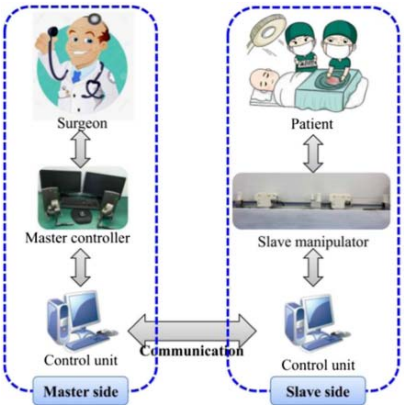

Fig. 1. Overall structure of the master-slave VIS robotic system [10]

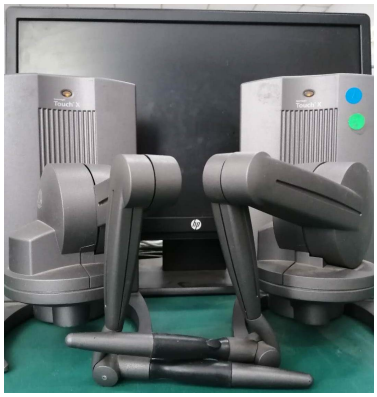

Fig. 2. Master manipulator

B. Salve manipulator

The slave manipulator is operated according to the introductions from the master side, which is the executive side, including the movement of real guide wire and catheter. The manipulator in the Fig.3 is developed by Guolab of Beijing institute of technology. This manipulator has three motion modules (module A, module B and module C) and two stationary support modules (module D and module E), and the relative position of the five modules is shown in Fig.3. And the Module A is the guide wire control unit, module B is catheter control unit, module C is a movable support device for the guide wire and catheter, module D is the stationary support for the catheter and module E is the stationary support for the guide wire. In addition, each module has clamping function.

In this manipulator, the guide wire control unit has the same operation method with the catheter control unit. So this part mainly presents the movement method of guide wire. And the cooperation of the module A~E are shown as follows. When the guide wire is only operated, and module A is activated by the motor A, and the module D is released at the same time. And the module C has the similar movement control method. And if guide wire and catheter are transmitted at the same time, there is an issue to cooperate them. And the module D and E will all release, and the module A~C will move according to the program. In addition, the relative position is also controlled by the information of the position sensor. And the force between the catheter/guide wire with the vascular is detected by force sensor, which are mounted on the module A and C.

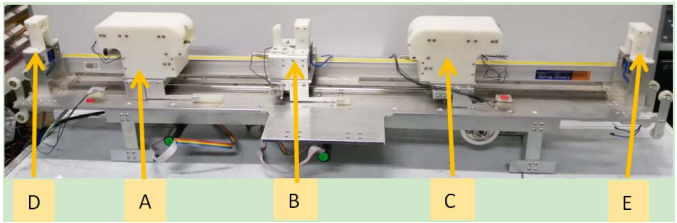

Fig. 3. Slave manipulator

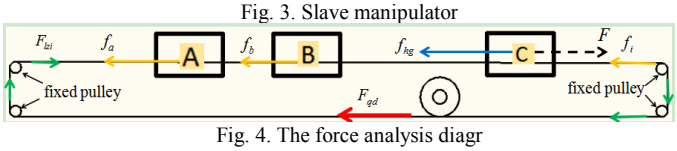

Fig. 4. The force analysis diagr

III. Displacement Model of Rope Driven

In this part, we research on the displacement model of the slave manipulator, and this model is used to calculate the theoretical displacement, this model is very helpful to ensure that the guide wire and catheter can move accurately to the target position. Therefore, the research on the displacement model of rope drive is important to the accurate control. In this slave manipulator, a rope-driven mechanics is applied to operate the catheter/guide wire and the movable support device, as shown in Fig.3. This mechanics is driven by the motor (386658, Maxon), which is controlled by the program, then motive power is transmitted to the guide wire control unit (module A), catheter control unit (module C) and movable support device (module B) through the rope, and the moving direction of rope is changed by the four fixed pulleys, as shown in Fig.4, which is a simplified force model diagram. In addition, the displacement model is established by analysing the related forces that influences the motion state of the guide wire/catheter control unit and movable support device. In this part, the friction between the wire rope with fixed pulley, the driving force of the motor, the inertial force of fixed pulley, the frictions between the rope with module A and B and the friction between the module A/B/C with leading rail are involved.

The displacement mathematical model is derived based on the Newton second law [shown in equation (1)], which presents the linear relationship between mass and acceleration.

$$F=m\ddot{x}_{out} \tag{1}$$

where the traction of module A/ B/C moving is F , is the mass of the module A/B/C, $\ddot{x}_{out}$ is acceleration of the module A/B/C. Therefore, the real output displacement (x_{out}) of A/B/C will be calculated by double integration of acceleration.

And the friction (f_i) between the wire rope with fixed pulley is calculated by the equation (2), it includes coulomb friction (f_{ic}) and viscous friction (f_{iv}), which are related with the torsion (F_T) and angular displacement (θ).

$$f_i = f_{ic}[F_T,\theta]\mathrm{sgn}(\dot{x}_{out}) + f_{iv}[F_T,\theta]\dot{x}_{out} \tag{2}$$

The output torque (T) of motor is calculated by the equation (3):

$$T = \frac{9550\times P}{n} \tag{3}$$

IV. Experiment And Results

The experiment platform is shown in the Fig 3. And the purpose of the experiment is to evaluate the performance of the displacement mathematical model presented in the Part III. Here the experiments are carried out in different velocity and given displacement, and a compensation model of the displacement is proposed based on the deviations.

A. Performance evaluation of the displacement model

$$F_{qd} = \frac{T}{R_{qd}} \tag{4}$$

where the P and are the power rating and rated speed of the motor respectively, and the equation (4) is applied to calculate the driving force (F_{qd}), and the R_{qd} is the driving pulley's radius.

The inertial force (F_{lzi}) of fixed pulley is calculated by equation (5), which is presented as follows:

$$F_{lzi} = J\ddot{\theta} = J\frac{2\pi n R_{qd}}{\Delta t R} \tag{5}$$

where the F_{lzi} is the active force, J and $\ddot{\theta}$ are the moment of inertia and angular acceleration of the fixed pulley respectively, and R is radius of fixed pulley.

The force balance equation of the rope-pulley system is shown in the equation (6):

$$F = F_{qd} - (f_{hg} + f_a + f_b + \sum_{i=1}^{4} f_i) + \sum_{i=1}^{4} F_{lzi} \tag{6}$$

where f_a and f_b are frictions between the rope with module A and B, respectively. And the friction is very little, so it will sometimes be ignored. And the $\sum_{i=1}^{4} f_i$ is the sum of friction between the rope with the four fixed pulley, the $\sum_{i=1}^{4} F_{lzi}$ is the sum of inertial force of four fixed pulley, and the f_{hg} is the friction between the module A/B/C with leading rail.

Therefore, the displacement mathematical model is derived by the equation (1) to (6) [shown in equation (7)] and in this equation, the $f_{hg} + f_a + f_b + \sum_{i=1}^{4} f_i$ is measured by the force sensor in the uniform state.

$$x_{out} = \begin{cases} x_{in} & , \textit{uniform state} \\ \iint \ddot{x}_{out}\mathrm{d}t^2 & , \textit{accelerated state} \end{cases} \tag{7}$$

in which

$$\ddot{x}_{out} = \frac{\dfrac{9550\ P}{nR_{qd}} - \left(f_{hg} + f_a + f_b + \sum_{i=1}^{4} f_i\right) + \sum_{i=1}^{4} F_{lzi}}{m} \tag{8}$$

In these experiments,58 values of the rope-driven system are outputted with different velocities, given displacements and acceleration, as shown in the TABLE I and TABLE II. And theoretically, the output values are equal to the given values in the uniform state and the accelerated state. And the output values of Table I and Table II are the measured values without any control algorithm. And these values are measured by the grating ruler (JCXE-DK, Guiyang Xintian Photoelectric Technology Co., Ltd.), and

the resolution is 0.0005mm.

TABLE I
THE REAL OUTPUT VALUES IN DIFFERENT DISPLACEMENT AND VELOCITY

Input displacement (mm) / Velocity (r/min)	50	100	150	200	250	300	350	400
35	47.7930	99.1205	149.5865	199.3880	250.0860	300.0540	350.0585	400.7470
70	47.8715	98.5215	148.8130	199.3720	250.0780	300.1425	350.4595	400.9070
105	47.8250	99.0690	148.9720	199.4975	251.0715	300.1000	350.3480	400.9560
140	47.7850	98.5605	149.2085	199.3905	249.8970	300.2665	350.4480	400.7480
175	47.9860	98.9990	149.0525	199.2695	250.0030	300.3490	350.1955	400.7500
210	47.9855	98.4845	148.9945	199.3965	250.1610	300.4655	350.3815	400.8775
Mean Measured Values (mm)	47.8743	98.7925	149.1045	199.3857	250.2161	300.2300	350.3152	400.6976
Deviation	-2.1257	-1.2075	-0.8955	-0.6143	0.2161	0.2296	0.3152	0.6976

TABLE II
THE REAL OUTPUT VALUES AND THEORETICAL VALUES IN DIFFERENT ACCERLERATION

Acceleration (mm/s^2)	1	2	3	4	5	6	7	8	9	10
Theoretical values (mm)	18	36	54	72	90	108	126	144	162	180
Measured values (mm)	17.0940	34.8935	52.5495	70.5825	88.4550	106.6205	125.0495	142.9105	160.8420	179.1265
Deviation	0.9060	1.1065	1.4505	1.4175	1.545	1.3795	0.9505	1.0895	1.158	0.8735

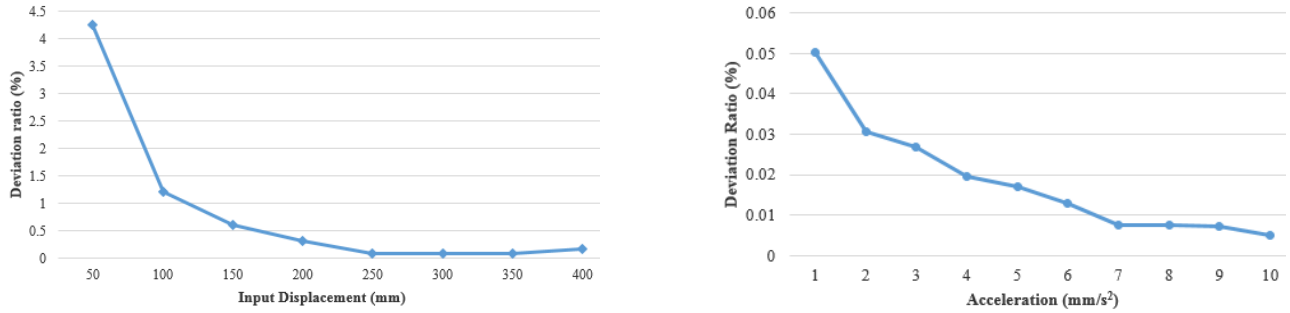

(a) (b)

Fig. 5. Deviation ratio in both states based on the model: (a) deviation ratio in uniform state; and (b) deviation ratio in accelerated state.

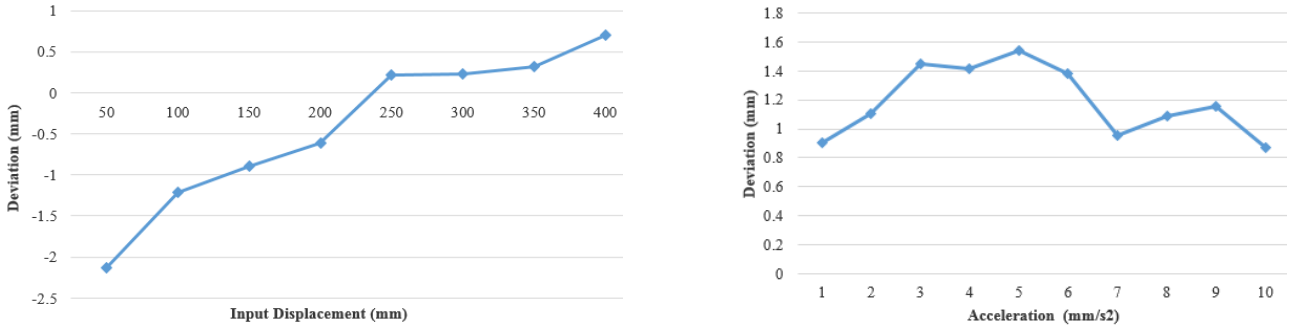

(a) (b)

Fig. 6. Deviation curve in both states: (a) the fitting curve in uniform state; and (b) the fitting curve in accelerated state.

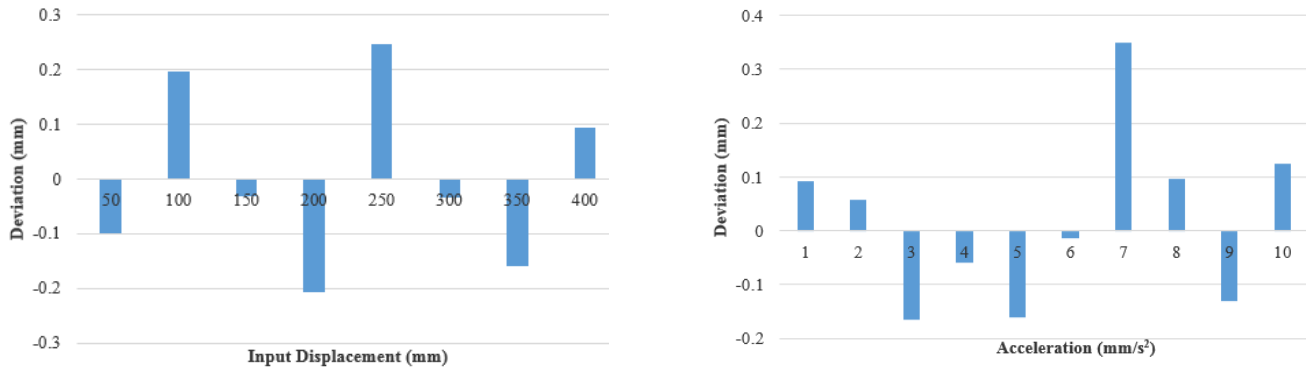

(a) (b)

Fig. 7. Deviation of the theoretical values and measured values in both states: (a) deviation in uniform state; and (b) deviation in accelerated state.

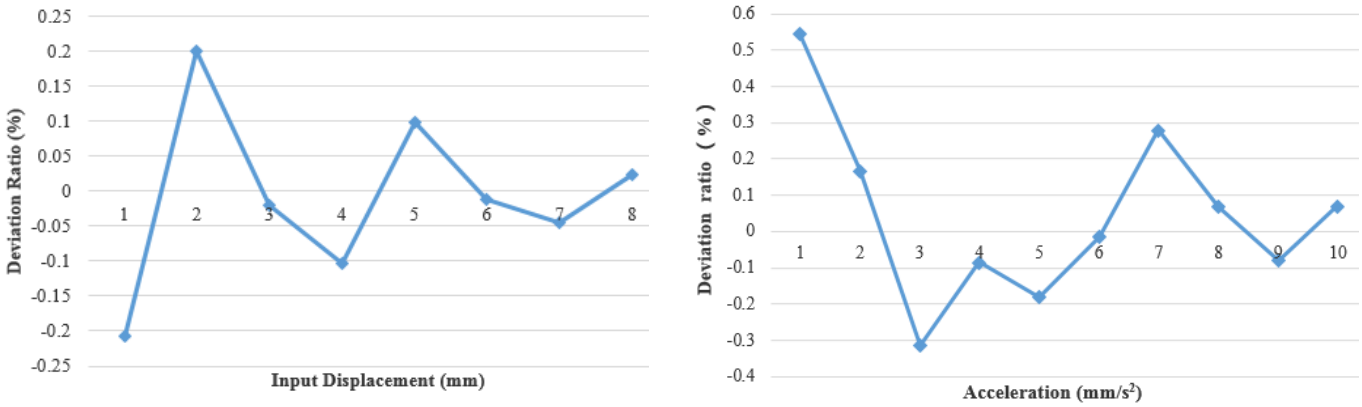

(a) (b)

Fig. 8. Deviation ratio in both states based on the updated model: (a) deviation ratio in uniform state; and (b) deviation ratio in accelerated state.

The deviation between the theoretical values and the measured values are shown in the TABLE I and TABLE II. In the TABLE I, the maximum deviation is -2.1257mm, the minimum deviation is 0.2161mm. In the TABLE II, the maximum deviation is 1.5450mm, the minimum deviation is 0.8735mm. And by rational analysis, the cause of the deviation is mainly the deformation of the rope. Of course, the deformation of the fixed pulleys also has influenced the precision, but it is very little. Therefore, it's necessary to further improve the precision of the theoretical model.

And the deviation ratio is calculated by the equation (9), as shown in the Fig. 5, it's easily found that the deviation is reduced when the given displacement is increased [Fig. 5(a)] or the acceleration is increased [Fig. 5(b)] in different states, in the uniform state [as shown in Fig. 5(a)], the biggest of the deviation ratio is 4.25%, and the smallest of the deviation ratio is 0.77%, and in the accelerated state [as shown in Fig. 5(b)], the biggest of the deviation ratio is 5.03%, the smallest of the deviation ratio is 0.48%.

$$R_a = \left| \frac{T - E}{T} \right| \times 100\% \tag{9}$$

where the theoretical values is represented by T, and E represents the measured values, and R_a represents the deviation ratio.

B. The proposed model of compensation

As mentioned above, it's necessary to further improve the precision of the theoretical model. Therefore, in this part, an error compensation algorithm is proposed based on the results of the last. And the compensation algorithm is proposed based on the deviation, and the fitting curve is depicted in the Fig. 6.

After that, the model of displacement is updated, as shown in the equation (10), and the x_{out}' is the real output displacement of the new model.

$$x_{out}' = \begin{cases} x_{in} + Dis_{arror1} & ,uniform\ \ state \\ \iint \ddot{x}_{out} \mathrm{d}t^2 - Dis_{arror2} & ,accelerated\ state \end{cases} \tag{10}$$

in which

$$Dis_{error1} = \frac{-0.0411 \times x^2}{2500} + \frac{0.7456 \times x}{50} - 2.731 \tag{11}$$

$$Dis_{error2} = -0.0232 \times x^2 + 0.2356 \times x + 0.7864 \tag{12}$$

$$\ddot{x}_{out} = \frac{9550P}{nR_{qd}m} - \frac{\left(f_{hg} + f_a + f_b + \sum_{i=1}^{4} f_i\right) + \sum_{I=1}^{4} F_{lzi}}{m} \quad (13)$$

And the same values with the last experiment are used to evaluate the performance of new model. And in both states, the deviation between the updated theoretical values and the measured values are shown in the Fig. 7. In uniform state, the maximum and minimum deviations are respectively 0.2466mm and -0.0314mm, and in accelerated state, the maximum deviation is 0.3483mm, the minimum deviation is -0.0147mm.

And comparing the deviation values of the new model with the initial model, as shown in the Fig. 8, the precision is improved largely, which is calculated by the equation (14), and in the uniform state [as shown in Fig. 8(a)], the maximum deviation ratio is 0.21%, the minimum deviation ratio is 0.05%, and in the accelerated state [as shown in Fig. 8(b)], the maximum deviation ratio is 0.55%, the minimum deviation ratio is 0.01%. Therefore, the new model can improve the precision of the displacement more effectively.

$$R_a^{'} = \left|\frac{T^{'} - E}{T^{'}}\right| \times 100\% \quad (14)$$

where the theoretical values calculated by the new model is represented $T^{'}$ by and $R_a^{'}$ is represent the deviation ratio.

V. Conclusion And Future Work

In this paper, the displacement model of the rope-driven method of the guide wire/catheter and movable support device is established. This model's performance is evaluated by the experiments. And there is a certain deviation between the theoretical values with the real output values. Therefore, in order to improve the positioning precision further, a compensation algorithm is proposed based on the deviations. Meanwhile, by comparing the precision of the new model with the initial, the new model can improve the positioning precision efficiently. And in the future study, the rotational movement mathematical model of the guide wire/catheter will be studied.

Acknowledgement

This research is partly supposed by National High-tech R&D Program (863 Program) of China (No.2015AA043202), and the National Key Research and Development Program of China (2017YFB1304401).

References

[1] L. Zhang, S. Guo, Yu H, et al, "Performance evaluation of a strain-gauge force sensor for a haptic robot-assisted catheter operating system," Microsystem Technologies, vol. 23, no. 10, pp. 5041-5050, 2017.

[2] J. Guo, S. Guo, Y. Yu, "Design and characteristics evaluation of a novel teleoperated robotic catheterization system with force feedback for vascular interventional surgery," Biomedical Microdevices, vol. 18, no. 5, pp. 76-91, 2016.

[3] Y. Wang, S. Guo, Tamiya T, et al, "A virtual□reality simulator and force sensation combined catheter operation training system and its preliminary evaluation," The International Journal of Medical Robotics and Computer Assisted Surgery, vol. 13, no. 3, DOI: 10.1002/rcs.1769, 2016.

[4] Y. Song, S. Guo, X. Yin, et al, "Design and performance evaluation of a haptic interface based on MR fluids for endovascular tele-surgery," Microsystem Technologies, vol. 24, no. 2, pp. 909-918, 2017.

[5] G. Weisz, D. C. Metzger, R. P. Caputo, et al, "Safety and Feasibility of Robotic Percutaneous Coronary Intervention," Journal of the American College of Cardiology, vol. 61, no. 15, pp. 1596-1600, 2013.

[6] K. Wang, B. Chen, Q. Lu, et al, "Design and Performance Evaluation of Real-time Endovascular Interventional Surgical Robotic System with High Accuracy," Int J Med Robotics Comput Assist Surg, vol. 14, no. 5, DOI: 10.1002/rcs.1915, 2018.

[7] Y. Song, S. Guo, X.Yin, et al, "Performance evaluation of a robot-assisted catheter operating system with haptic feedback," Biomedical Microdevices, vol. 20, no. 2, pp. 50-65, 2018.

[8] S. Hao, C. Wang, L. Xie, "A novel remote-controlled robotic system for cerebrovascular intervention," Int J Med Robotics Comput Assist Surg, vol. 14, no. 6, DOI: 10.1002/rcs.1943, 2018.

[9] X. Bao, S. Guo, N. Xiao, et al, "Operation evaluation in-human of a novel remote-controlled vascular interventional robot," Biomedical Microdevices, vol. 20, no. 2, pp. 34-46, 2018.

[10] X. Bao, S. Guo, N. Xiao, et al, "A cooperation of catheters and guidewires-based novel remote-controlled vascular interventional robot," Biomedical Microdevices, vol. 20, no. 1, pp. 20-38, 2018.

[11] X. Bao, S. Guo, N. Xiao, et al, "Compensatory force measurement and multimodal force feedback for remote-controlled vascular interventional robot," Biomedical Microdevices, vol. 20, no. 3, pp. 74-84, 2018.

[12] Y. Zhao, S. Guo, Y. Wang, et al, "A CNNs-based Prototype Method of Unstructured Surgical State Perception and Navigation for an Endovascular Surgery Robot," Medical & Biological Engineering & Computing, in press, 2019.

[13] S. Guo, Y. Song, X. Yin, Linshuai Zhang, et al, "A Novel Robot-Assisted Endovascular Catheterization System with Haptic Force Feedback," The IEEE Transactions on Robotics, DOI: 10.1109/TRO.2019.2896763, 2019.

[14] X. Bao, S. Guo, N. Xiao, L. Shi, "Design and Evaluation of Sensorized Robot for Minimally Vascular Interventional Surgery," Microsystem Technologies, DOI: 10.1007/s00542-019-04297-3, 2019.

[15] X. Yin, S. Guo, Y. Song, "Magnetorheological fluids actuated haptic-based teleoperated catheter operating system," Micromachines, vol. 9, no. 9, DOI: 10.3390/mi9090465, 2018.

[16] J. Guo, S. Guo, "A Marker-based Contactless Catheter-sensing Method to Detect Surgeons' Operations for Catheterization Training Systems," Biomedical Microdevices, vol. 20, no. 3, DOI: 10.1007/s10544-018-0321-5, 2018.

[17] S. Guo, X. Cai, B. Gao, "A Tensor-Mass Method-based Vascular Model and its Performance Evaluation for Interventional Surgery Virtual Reality Simulator," The International Journal of Medical Robotics and Computer Assisted Surgery, vol. 14, no. 6, DOI: 10.1002/rcs.1946, 2018.

[18] S. Guo, Y. Wang, N. Xiao, Y. Li, Y. Jiang, "Study on Real-time Force Feedback with a Master-slave Interventional Surgical Robotic System," Biomedical Microdevices, vol. 20, no. 2, DOI: 10.1007/s10544-018-0278-4, 2018.

[19] L. Zhang, S. Guo, H. Yu, Y. Song, et al, "Design and performance evaluation of collision protection-based safety operation for a haptic robot-assisted catheter operating system," Biomedical Microdevices, vol. 20, no. 2, pp. 22-35, 2018.

[20] Y. Wang, S. Guo, N. Xiao, et al, "Online Measuring and Evaluation of Guidewire Inserting Resistance for Robotic Interventional Surgery Systems," Microsystem Technologies, vol. 24, no. 8, pp. 3467-3477, 2018.

[21] J. Guo, X. Jin, S. Guo, "Study of the Operational Safety of a Vascular Interventional Surgical Robotic System," Micromachines, vol. 9, no. 3, DOI:10.3390/mi9030119, 2018.

[22] M. A. Tavallaei, D. Gelman, M. K. Lavdas, et al, "Design, development and evaluation of a compact telerobotic catheter navigation system," Int J Med Robotics Comput Assist Surg, vol. 12, no. 3, pp. 442-452, 2016.